*Journal of Fluorescence, Vol. 14, No. 1, January 2004 (©2004)*

# Global Analysis of Steady-State Energy Transfer Measurements in Membranes: Resolution of Structural and Binding Parameters

**Yegor A. Domanov,[1,3] Galina P. Gorbenko,[1] and Julian G. Molotkovsky[2]**

*Received July 29, 2003; accepted September 29, 2003*

A method has been developed allowing structural and binding parameters to be recovered by global analysis of two-dimensional array of steady-state RET data in the special case where energy acceptors distribute between aqueous and lipid phases while donors are embedded in the membrane at a known depth. To test the validity of this approach, correlation and error analyses have been performed using simulated data. To exemplify the method application to the membrane studies, energy transfer from anthrylvinyl-labeled phosphatidylcholine incorporated into mixed phosphatidylcholine/cardiolipin unilamellar vesicles to heme group of cytochrome c is analyzed.

**KEY WORDS:** Resonance energy transfer; membrane systems; global analysis; structural and binding parameters.

## INTRODUCTION

Resonance energy transfer (RET) has found numerous applications in membrane studies providing information on proximity relationships [1,2], molecular clustering [3], lipid domain formation [4,5], protein adsorption [6–9], etc. An extensive use of RET technique is determined by its ability to give unique structural information, complementary to that obtained by other powerful physical methods such as X-ray and neutron scattering, NMR, and cryoelectron microscopy [2]. Among the main advantages of RET approach to structural characterization of membrane systems are: use of diluted samples, monitoring of the membrane processes under physiological conditions, high sensitivity, and relative simplicity of the experiment.

In the present paper, we consider a special case of the steady-state RET application to model membrane systems where energy acceptors distribute between aqueous and lipid phases while donors are embedded in the membrane at a known depth (e.g., by means of phospholipid covalent labeling). In principle, measurements in this format can provide information on the transverse location of acceptor/acceptor-labeled molecule in the lipid bilayer. However, the analysis and interpretation of experimental data may be complicated by the fact that RET efficiency in the membrane depends both on the transverse distance separating the donor and acceptor arrays, and on the acceptor surface concentration, which is in turn determined by the extent of acceptor binding to the membrane. Indeed, it is often difficult to differentiate the contributions of these two factors to the overall transfer efficiency [10]. This obstacle can be overcome by estimating binding parameters for the studied system in a separate binding assay, and then recalculating the amount of bound acceptor corresponding to the conditions of RET experiment. There are two main groups of binding assays [8]: those where bound and free ligand undergo physical separation, and indirect ones, taking advantage of the changes in a particular spectral property (e.g., absorbance, fluorescence intensity, anisotropy) upon binding. The former group of methods includes centrifugation or gel filtration, which have

[1] Department of Biological and Medical Physics, V. N. Karazin Kharkiv National University, Kharkiv, Ukraine.
[2] Laboratory of Lipid Chemistry, Shemyakin-Ovchinnikov Institute of Bioorganic Chemistry, Russian Academy of Sciences, Moscow, Russia.
[3] To whom correspondence should be addressed at 39 pr. Lenina, Apt. 96, Kharkiv 61072, Ukraine. E-mail: domanov@pochta.ru



1053-0509/04/0100-0049/0 

serious drawbacks: separation causes shift of equilibrium between free and bound ligand, the assays are often carried out in the range of concentrations that differ significantly from those used in RET experiment, the methods are time- and labor-consuming. Spectroscopic techniques, although very sensitive and applicable under the same conditions as RET, assume certain relation between the change in spectral parameter and the amount of bound ligand, which is not always direct and unambiguous.

Given the above complications, the question arises whether it is possible to resolve structural parameter (transverse location of membrane-bound acceptor) and binding parameters using steady-state RET measurements alone. In the present paper we propose an experimental design and data treatment methodology allowing both structural and binding parameters to be determined with high accuracy and statistical significance. The approach is based on global analysis (GA) of two-dimensional array of energy transfer data obtained by varying both total acceptor concentration and lipid concentration. The analysis is made possible by combining adequate model of membrane RET with appropriate binding model. To validate this approach to parameter resolution, we use simulated data and analyze associated error surfaces ($\chi^2$-statistic vs. estimated parameters) and coefficients of parameter cross-correlation. As an example of application, energy transfer from anthrylvinyl-labeled phosphatidylcholine incorporated into mixed phosphatidylcholine/cardiolipin unilamellar vesicles to heme group of cytochrome *c* is analyzed.

## THEORY

In this section, we briefly describe theoretical models involved in the global analysis scheme presented here. The choice of these models is dictated by their relative simplicity on the one hand, and possibility to illustrate principal features of the proposed approach on the other. Consider a model system where lipid bilayer-embedded donor and bound acceptor are characterized by certain transverse locations in the membrane. In other words, donors and acceptors are confined to two parallel planes separated by a distance $d_a$. Suppose further that donors and acceptors are randomly distributed over their respective planes. According to the theory described in more detail earlier [11–13], the interplane separation $d_a$ is related to the relative quantum yield of donor, $Q_r$, by the following relationships:

$$Q_r = \frac{Q_{DA}}{Q_D} = \int_0^\infty e^{-\lambda}(I(\lambda))^N \, d\lambda, \qquad (1)$$

where $Q_D$ and $Q_{DA}$ are the donor quantum yields in the absence and presence of acceptor, respectively, $\lambda = t/\tau_D$ is the dimensionless time, $\tau_D$ is the lifetime of the donor in the absence of acceptor, $N$ is the number of acceptor molecules in the vicinity of the donor, and $I(\lambda)$ is the additional donor decay term due to energy transfer to each of the surrounding acceptors:

$$I(\lambda) = \int_{d_a}^{R_d} \exp\left[-\lambda(R_0/R)^6\right] \cdot W(R)\, dR, \qquad (2)$$

where $R_0$ is the Förster distance, $R_d$ is the distance beyond which energy transfer is negligible ($R_d \geq 3R_0$), and $W(R)dR$ is the probability of finding an acceptor at the distance between $R$ and $R + dR$ from the donor. The form of the expressions for $W(R)$ and $N$ depends on the system geometry, and in the simplest case considered here they are given by:

$$W(R) = \frac{2R}{R_d^2 - d_a^2}; \; N = \pi C_A^s \left(R_d^2 - d_a^2\right). \qquad (3)$$

Here $C_A^s$ is the acceptor surface concentration related to the molar concentrations of bound acceptor, $B$, and accessible lipid, $L_{acs}$:

$$C_A^s = \frac{B}{L_{acs} \sum f_j S_j}, \qquad (4)$$

$f_j$ and $S_j$ being the mole fraction and mean area per molecule of the $j$-th lipid species constituting the membrane, respectively.

Note that to apply the above formalism one needs to know the concentration of bound acceptor $B$, which determines the surface acceptor concentration $C_A^s$ (Eq. (4)), and hence the relative quantum yield of donor $Q_r$. To relate the amount of bound acceptor $B$ to the total acceptor concentration, $A$, and accessible lipid concentration $L_{acs}$, one should employ an appropriate binding model. To simplify further analysis we use here conventional Langmuir model:

$$K_d = \frac{B}{(A-B)(L_{acs}/n - B)},$$
$$B = \frac{1}{2}\left[A + \frac{L_{acs}}{n} + K_d - \sqrt{\left(A + \frac{L_{acs}}{n} + K_d\right)^2 - 4\frac{AL_{acs}}{n}}\right], \qquad (5)$$

where $K_d$ is the equilibrium dissociation constant, and $n$ is the binding stoichiometry.

By combining Eqs. (1)–(5) one obtains the relative quantum yield as a function of five variables: $Q_r = f(A, L_{acs}; n, K_d, d_a)$. The two of them, $A$ and $L_{acs}$, are independent variables that can be varied in the experiment ($L_{acs}$ depends on the total lipid concentration, $L$,

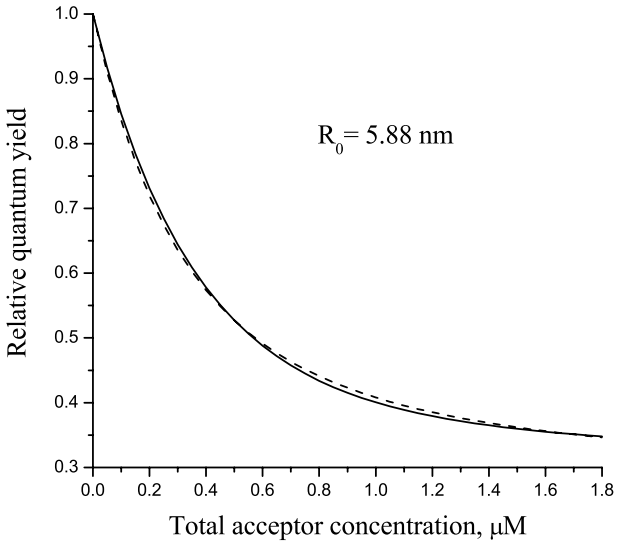


**Fig. 1.** Relative quantum yield of donor as a function of total acceptor concentration calculated for total lipid concentration $L = 150\ \mu$M and two different sets of parameters: $n = 100$, $K_d = 0.2\ \mu$M, $d_a = 5.0$ nm—solid line, $n = 195$, $K_d = 0.4\ \mu$M, $d_a = 3.0$ nm—dashed line.

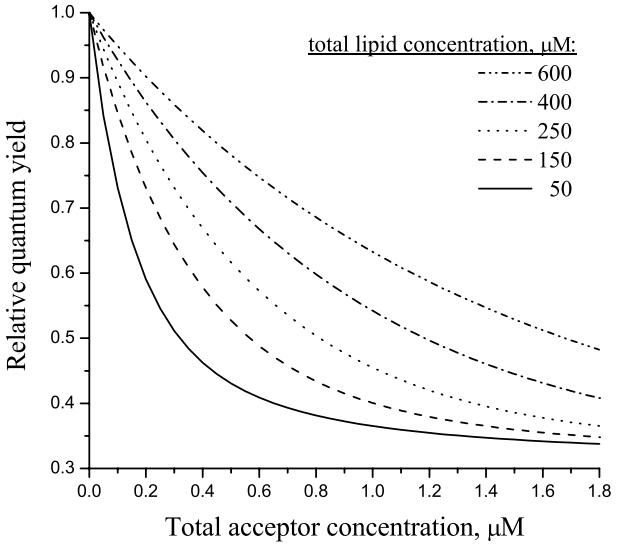


**Fig. 2.** Dependence of quenching profiles on total lipid concentration, $n = 100$, $K_d = 0.2\ \mu$M, $d_a = 5.0$ nm, $R_0 = 5.88$ nm.

and the type of model system; e.g., for large unilamellar vesicles and non-permeating acceptor it is assumed that $L_{acs} = 0.5L$). $n$, $K_d$, and $d_a$ are unknown parameters to be determined by least-squares analysis of experimental data.

A typical dependence of the relative quantum yield on the total acceptor concentration is shown in Fig. 1 (solid curve). The calculation was performed at a fixed total lipid concentration $L = 150\ \mu$M, and the following values of parameters: $n = 100$, $K_d = 0.2\ \mu$M, $d_a = 5.0$ nm. Importantly, simulations show that the set of parameters providing this particular dependence is not unique. As an example, the dashed curve in Fig. 1 was calculated using $n = 195$, $K_d = 0.4\ \mu$M, $d_a = 3.0$ nm, a completely different set of parameters. As can be seen from Fig. 1, the two curves are virtually indistinguishable from each other. This phenomenon, known as parameter cross-correlation [14,15], is frequently encountered in biophysical and biochemical investigations. In some RET applications, one would be content with *relative* changes in acceptor surface coverage and/or position upon varying the experimental conditions (instead of the *exact* values of the parameters). However, severe cross-correlation of the fitting parameters makes it impossible to judge whether the changes in relative quantum yield of donor result from the variation of the acceptor transverse location or from the changes in its binding to the membrane. Therefore, it is necessary to ascertain what format of RET measurements permits structural and/or binding parameters to be determined unambiguously.

In the next section it is shown that the cross-correlation between the above three fitting parameters ($n$, $K_d$, $d_a$) can be overcome by the simultaneous analysis of a two-dimensional array of experimental data obtained by varying both total acceptor concentration and lipid concentration. Shown in Fig. 2 are quenching profiles calculated for five lipid concentrations and parameter values typical for protein-lipid interactions ($n = 100$, $K_d = 0.2\ \mu$M, $d_a = 5.0$ nm). As the lipid concentration increases, acceptor molecules distribute over a greater bilayer area resulting in the acceptor surface concentration decrease, and lowered energy transfer (rising curves in Fig. 2). It is this peculiarity of energy transfer dependence on total acceptor and lipid concentrations that makes it possible to resolve structural and binding parameters by global analysis of the expanded data array.

## RESULTS

### Simulations

To test the validity of the proposed approach in analyzing the steady-state RET data and to evaluate the accuracy and cross-correlation of recovered structural and binding parameters, computer simulations were employed. Relative quantum yield was calculated using Eqs. (1)–(5) for various combinations of total acceptor concentration ($A$) and total lipid concentration ($L$) within the ranges typical for RET experiments: $0 \le A \le 1.8\ \mu$M, $80 \le L \le 630\ \mu$M. Preset values of parameters $n$, $K_d$, and $d_a$ were used in the calculation. Gaussian noise

with a standard deviation of 0.015 was added to the calculated data to mimic experimental errors. Further analysis was performed in terms of the reduced $\chi^2$ statistic [16]:

$$\chi^2_{\mathrm{R}}(n, K_{\mathrm{d}}, d_{\mathrm{a}}) = \frac{1}{n_{\mathrm{A}} n_{\mathrm{L}} - 3} \times \sum_{i=1}^{n_{\mathrm{A}}} \sum_{j=1}^{n_{\mathrm{L}}} \frac{(Q_{\mathrm{r}}(A_i, L_j, n, K_{\mathrm{d}}, d_{\mathrm{a}}) - \mathrm{EXP}_{i,j})^2}{\sigma^2} \quad (6)$$

where $n_{\mathrm{A}}$ and $n_{\mathrm{L}}$ are the numbers of acceptor and lipid concentrations, respectively, $\mathrm{EXP}_{i,j}$ is the relative quantum yield simulated for the $i$-th acceptor concentration and $j$-th lipid concentration, $\sigma$ is the standard deviation.

Three characteristic RET datasets were considered: 1) Univariate data (1D data) obtained at a fixed lipid concentration by varying total acceptor concentration only (30 simulated data points); input values of parameters: $n = 100$, $K_{\mathrm{d}} = 0.2$ $\mu$M ($n$ and $K_{\mathrm{d}}$ corresponding to the saturable (with respect to $A$) binding in the specified ranges of concentrations), $d_{\mathrm{a}} = 5.0$ nm; $L = 158$ $\mu$M. 2) Two-dimensional data array (2D data) obtained by varying both lipid and total acceptor concentrations; input values of parameters: $n = 100$, $K_{\mathrm{d}} = 0.2$ $\mu$M (saturable binding), $d_{\mathrm{a}} = 5.0$ nm; 30 data points total: 5 lipid concentrations $\times$ 6 acceptor concentrations. 3) 2D data for the case of unsaturable binding; input values of parameters: $n = 30$, $K_{\mathrm{d}} = 5$ $\mu$M ($n$ and $K_{\mathrm{d}}$ corresponding to the linear/unsaturable (with respect to $A$) binding isotherms in the specified ranges of concentrations), $d_{\mathrm{a}} = 5.0$ nm; 30 data points total ($5L_j \times 6A_i$).

To assess how the quality and uniqueness of the least-squares fitting depend on the format of RET data we analyzed the projections of the corresponding error surfaces with respect to specific parameters (Fig. 3A–C). An error surface is known to be a $\chi^2$ statistic for a given dataset plotted against optimized parameters. Error surfaces are now increasingly used in data analyses, providing the most adequate way to estimate uncertainties in the parameters derived from least-squares fitting [16–18]. The curves in Fig. 3A–C were generated by fixing one parameter at a series of values, and performing a nonlinear minimization, allowing the remaining parameters to vary until the minimum of $\chi^2_R$ is reached. The series of minimum $\chi^2_R$ values possible over a particular range of the fitting parameter ($d_{\mathrm{a}}$, $K_{\mathrm{d}}$, or $n$) was recorded for each of the three formats of RET data. The error surface projections for the univariate data (1D data) depicted by dashed curves in Fig. 3 are seen to be very ill-defined, i.e. show no clear minimum. In contrast, the two-dimensional data (2D data) result in well-defined error surfaces, with distinct and relatively narrow minima close to the input values of the parameters. Solid and dotted curves in Fig. 3 correspond to the

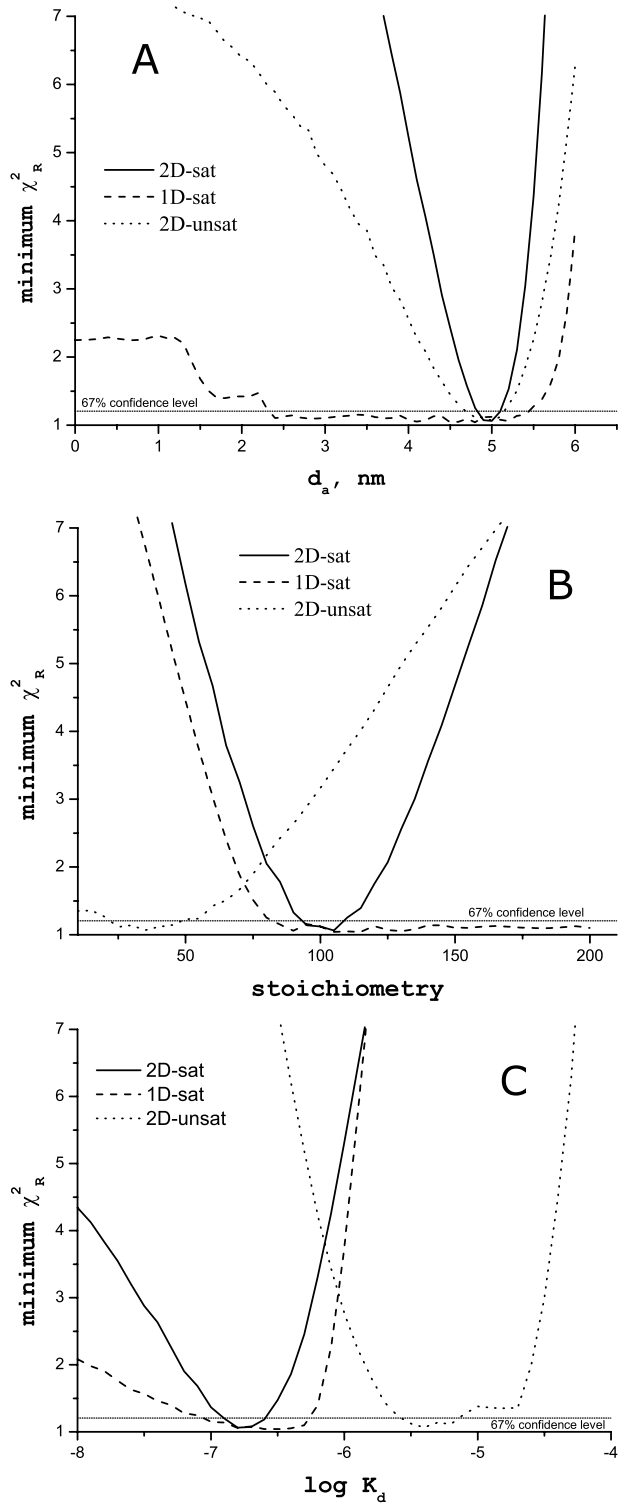


**Fig. 3.** Projections of the error surfaces with respect to the fitting parameters ($d_{\mathrm{a}}$, $n$, $K_{\mathrm{d}}$) for the different types of data: 1D data (saturable binding)—dashed lines, 2D data (saturable binding)—solid lines, 2D data (unsaturable binding)—dotted lines. Panel A, dependence on $d_{\mathrm{a}}$; panel B, dependence on $n$; panel C, dependence on $K_{\mathrm{d}}$.

2D data simulated for the conditions of saturable and unsaturable binding, respectively. Note that in the case of unsaturable (within the experimental range of $A$) binding minima of the error surface projections for both binding *and structural* parameters are broader than those observed in the case of saturable binding.

Also shown in Fig. 3 are 67% confidence levels as determined by $F$-statistic [16]. Confidence intervals are obtained as abscissas of intersection of the confidence level with corresponding error surface projections. For example, confidence intervals for the donor-acceptor interplane separation ($d_a$) are as follows: $2.3 < d_a < 5.4$ nm for the 1D data, $4.8 < d_a < 5.1$ nm for the 2D data (saturable binding), and $4.7 < d_a < 5.2$ nm for the 2D data (unsaturable binding). As can be seen from Fig. 3B and C, similar tendencies in the changes of confidence intervals hold for the binding parameters, $K_d$ and $n$. Clearly, univariate data analysis can hardly provide any satisfactory estimates of the parameters, while global analysis of the two-dimensional data array allows the parameters to be determined with high accuracy and statistical significance.

To further analyze the origins of such dramatic difference in the accuracy of least-squares estimation, coefficients of cross-correlation for the different formats of experimental data were calculated. A coefficient of cross-correlation for a pair of fitting parameters shows the extent to which the increase in $\chi^2$ caused by a variation in one parameter can be compensated for by a variation in the other one [15]. The values of a cross-correlation coefficient vary within $\pm 1$, with zero indicating no cross-correlation between the parameters. It is generally accepted that a cross-correlation above $\sim 0.95$, in absolute value, indicates that the parameters are highly correlated, and in this case the model and/or experimental design should be reconsidered [15,19].

Here we make use of the two types of coefficients: general and partial coefficients of cross-correlation. General coefficients of cross-correlation reflect mutual influence of the two parameters, say, $\alpha_1$ and $\alpha_2$, when the remaining parameters are allowed to vary. In this way, general coefficients of cross-correlation are also sensitive to all higher order correlations mediated by the remaining parameters—it is a "net" characteristic. On the contrary, partial coefficients of cross-correlation characterize direct correlation of the two parameters when all remaining parameters are considered as fixed. Calculation of the cross-correlation coefficients is based on the matrix of partial derivatives of the fitting function, $G$, with respect to the fitting parameters, $\alpha_l$ [15]:

$$J_{k,l} = \frac{\partial G(\alpha_1, \alpha_2, \ldots, \mathbf{X_k})}{\partial \alpha_l}, \tag{7}$$

**Table I.** General Coefficients of Cross-Correlation

| Type of data | Pair of parameters | | |
|---|---|---|---|
| | $n - K_d$ | $d_a - n$ | $d_a - K_d$ |
| 1Ddata (saturable binding) | 0.911 | −0.973 | −0.979 |
| 2Ddata (saturable binding) | −0.360 | −0.336 | −0.703 |
| 2Ddata (unsaturable binding) | −0.968 | 0.101 | −0.340 |

where $\mathbf{X_k}$ is the vector of independent variables in the $k$-th experimental point. The general coefficient of cross-correlation, $s_{l,m}$, between $l$-th and $m$-th parameter is defined as [20]:

$$s_{l,m} = \frac{[(\mathbf{J^T J})^{-1}]_{lm}}{\sqrt{[(\mathbf{J^T J})^{-1}]_{ll} \cdot [(\mathbf{J^T J})^{-1}]_{mm}}} \tag{8}$$

where $\mathbf{J^T}$ is the transpose of $\mathbf{J}$, and $-1$ refers to the matrix inversion. Corresponding partial coefficient, $r_{l,m}$, is defined as:

$$r_{l,m} = \frac{-(\mathbf{J^T J})_{lm}}{\sqrt{(\mathbf{J^T J})_{ll} \cdot (\mathbf{J^T J})_{mm}}} \tag{9}$$

General and partial coefficients of cross-correlation calculated for the different types of RET data are presented in Tables I and II, respectively. It appears that in the case of the univariate data analysis the correlation between the structural and binding parameters is very high ($\sim 0.98$). It is this correlation that leads to the ill-defined error surface for the univariate data: numerous combinations of parameters give essentially identical $\chi^2_R$ statistic (Fig. 3, dashed curves). Advantage of the global analysis of two-dimensional data is evidenced by significantly smaller values of the parameter cross-correlation coefficients (Tables I and II). Thus, simultaneous determination of structural and binding parameters becomes possible due to significantly reduced cross-correlation between the parameters when 2D-array of RET measurements is globally analyzed.

Data in Tables I and II also demonstrate that the extent of parameter cross-correlation, and hence the accuracy of parameter estimation by 2D-data global analysis depend on the mode of acceptor binding. If RET experiment is

**Table II.** Partial Coefficients of Cross-Correlation

| Type of data | Pair of parameters | | |
|---|---|---|---|
| | $n - K_d$ | $d_a - n$ | $d_a - K_d$ |
| 1Ddata (saturable binding) | −0.904 | −0.972 | −0.978 |
| 2Ddata (saturable binding) | −0.889 | −0.887 | −0.937 |
| 2Ddata (unsaturable binding) | −0.998 | −0.971 | −0.974 |

carried out in the ranges of lipid and acceptor concentrations where acceptor binding is unsaturable, the correlation between parameters is seen to be high even in the case of 2D data.

It should be noted that the cross-correlation between the parameters of a nonlinear model, which is the case here, is a function of the specific parameters values [15]. Therefore, the analyses performed here for the two characteristic sets of parameters (modeling saturable and unsaturable binding) cannot themselves rigorously prove the superiority of our global analysis approach in general. However, similar simulations performed for different input values of $n$, $K_d$ and $d_a$ (data not shown) yielded similar results.

## Experimental Data Analysis

As an illustration of the proposed global analysis approach, an example of real experimental data is given and analyzed. Fluorescent labeled phospholipid, 1-acyl-2-[12-(9-anthryl)-11-*trans*-dodecenoyl]-*sn*-glycerophosphocholine (AV-PC) [21] was used as energy donor, while heme group of water-soluble protein cytochrome *c* (oxidized form) served as acceptor. AV-PC was incorporated (at a molar ratio <0.01) into unilamellar lipid vesicles composed of egg phosphatidylcholine and beef heart cardiolipin (10 mol%). Butylated hydroxytoluene (5 mol%) was added to the membranes to prevent lipid peroxidation. Fluorescence measurements were performed with Hitachi M-850 spectrofluorimeter. AV-PC fluorescence was excited at 368 nm, and registered at 434 nm (emission maximum). Slit widths were 5 nm. Förster radius ($R_0$) for the pair AV-PC/cytochrome *c* was calculated to be 4.7 nm. Relative quantum yield of AV-PC was calculated as a ratio of intensities in the presence and in the absence of acceptor. Figure 4 shows relative quantum yield of AV-PC as a function of the total cytochrome *c* concentration, recorded at five different concentrations of lipid (data points with error bands). Solid lines in Fig. 4 represent best fit of the data by the global analysis procedure yielding the following estimates of the fitting parameters: $d_a = 3.51$ nm, $K_d = 0.28$ $\mu$M, $n = 27$. Corresponding 67% confidence intervals were found to be: $3.42 < d_a < 3.60$ nm, $0.20 < K_d < 0.37$ $\mu$M, and $25 < n < 29$.

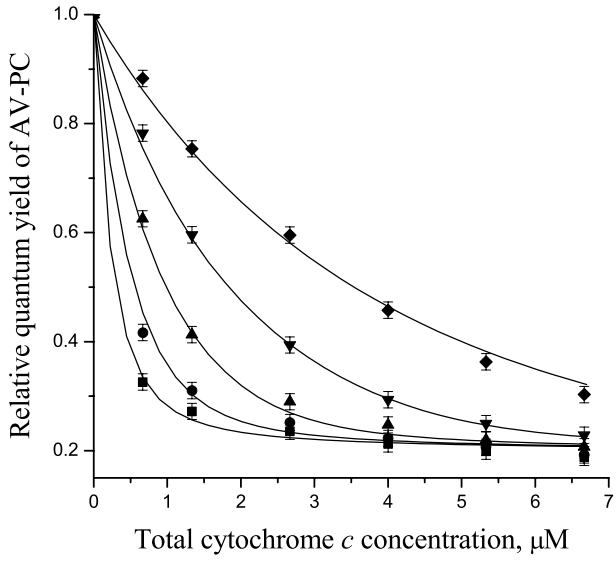


**Fig. 4.** Global fit of experimental RET data for cytochrome *c* interaction with the AV-PC-doped lipid vesicles. $R_0 = 4.7$ nm. Total lipid concentrations (bottom to top, $\mu$M): 29, 71, 143, 285, 571.

## DISCUSSION

In this paper we proposed a new methodology for the analysis of steady-state RET measurements in membranes based on global least-squares fit of two-dimensional data array obtained by varying both lipid and acceptor concentrations. It was shown that in the special case where energy transfer occurs from donors localized in the membrane at a known depth to acceptors distributed between aqueous and lipid phases, this type of analysis can provide unambiguous information on both binding parameters and transverse location of acceptor in the membrane.

Global analysis is now widely used in biophysical and biochemical studies as a powerful tool for quantitative interpretation of experimental results. A great number of examples evidence fruitfulness of global analysis applied to fluorescence data. Particularly, in time-resolved RET studies GA allowed to distinguish between intramolecular distance distributions and conformational dynamics in macromolecules [17], to recover multiple fluorescence lifetimes in protein [22], and to resolve fluorescence decay parameters and dimensionality of fluorophore distribution in model membranes [23]. Applied to steady-state RET data, GA permitted simultaneous determination of dissociation constant, stoichiometry of protein binding to membrane, and distance of closest approach between fluorescent labeled protein and lipid-bound probe [24]. In the main, the data treatment procedure employed by Chen and Lentz [24] is similar to the approach presented here, but the analysis was performed for a different case where acceptors are confined to the lipid bilayer while donors partition between aqueous and lipid phases.

Analysis of the data presented here led us to several ideas regarding the optimal design of RET experiment and

perspectives of using steady-state RET in membrane studies. Firstly, to ensure appreciable energy transfer, Förster distance ($R_0$) for the donor-acceptor pair employed should be of the order of $d_a$, the donor-acceptor interplane separation. Secondly, if Langmuir binding model (or any model with more than one fitting parameter) is used, one should choose the ranges of lipid and acceptor concentrations that provide the widest limits for the total acceptor-to-lipid molar ratio possible in RET experiment, so that the region of saturation would be covered. The accuracy of both binding and structural parameter estimation decreases if the experiment is carried out in the concentration range where acceptor binding is unsaturable with respect to the total acceptor concentration, or in the case where binding is linear with respect to lipid concentration (the case where the acceptor surface density is independent of the lipid concentration). The requirement of the wide concentration range is in accordance with the recent conclusion by Johnson [15] that the wider the range of independent variables, the lower the cross-correlation of fitting parameters. Finally, the presented approach provides a basis for deriving structural information and binding characteristics within the framework of more sophisticated RET and binding models taking into account peculiar membrane processes such as lipid domain formation, protein aggregation, etc. Thus, steady-state RET data globally analyzed in terms of the proposed approach are expected to give more profound quantitative information on a variety of membrane phenomena.

## ACKNOWLEDGMENTS

We wish to thank Dr. M. Ye. Tolstorukov (NCI/NIH) for his help with literature on data analysis. We are also very grateful to Prof. Yu. V. Kholin for helpful discussions on parameter correlation, and to Drs A. D. Roshal and A. O. Doroshenko for the use of the fluorescence facilities (Kharkiv National University).

## REFERENCES

1. J. Szöllösi, S. Damjanovich, S. A. Mulhern, and L. Trón (1987). Fluorescence energy transfer and membrane potential measurements monitoring dynamic properties of cell membranes: A critical review. *Prog. Biophys. Mol. Biol.* **49**, 65–87.
2. P. R. Selvin (1995). Fluorescence resonance energy transfer. *Meth. Enzymol.* **246**, 300–334.
3. J. Matko, M. Edidin (1997). Energy transfer methods in detecting molecular clusters on cell surfaces. *Meth. Enzymol.* **278**, 444–462.
4. S. Pedersen, K. Jørgensen, T. R. Bækmark, and O. G. Mouritsen (1996). Indirect evidence for lipid-domain formation in the transition region of phospholipid bilayers by two-probe fluorescence energy transfer. *Biophys. J.* **71**, 554–560.
5. L. M. S. Loura, A. Fedorov, and M. Prieto (2001). Fluid-fluid membrane microheterogeneity: A fluorescence resonance energy transfer study. *Biophys. J.* **80**, 776–788.
6. M. Subramanian, A. Jutila, and P. K. Kinnunen (1998). Binding and dissociation of cytochrome *c* to and from membranes containing acidic phospholipids. *Biochemistry* **37**, 1394–1402.
7. S. D. Zakharov, M. Lindeberg, and W. A. Cramer (1999). Kinetic description of structural changes linked to membrane import of the colicin E1 channel protein. *Biochemistry* **38**, 11325–11332.
8. J. B. Heymann, S. D. Zakharov, Y.-L. Zhang, and W. A. Cramer (1996). Characterization of electrostatic and nonelectrostatic components of protein-membrane binding interactions. *Biochemistry* **35**, 2717–2725.
9. T. J. T. Pinheiro, G. A. Elöve, A. Watts, and H. Roder (1997). Structural and kinetic description of cytochrome *c* unfolding induced by the interaction with lipid vesicles. *Biochemistry* **36**, 13122–13132.
10. J. Eisinger, J. Flores, and R. M. Bookchin (1984). The cytosol-membrane interface of normal and sickle erythrocytes. Effect of hemoglobin deoxygenation and sickling. *J. Biol. Chem.* **259**, 7169–7177.
11. P. Wolber, B. Hudson (1979). An analytic solution to the Förster energy transfer problem in two dimensions. *Biophys. J.* **28,** 197–210.
12. G. P. Gorbenko and Ye. A. Domanov (2002). Energy transfer method in membrane studies: Some theoretical and practical aspects. *J. Biochem. Biophys. Methods* **52**, 45–58.
13. Ye. A. Domanov and G. P. Gorbenko (2002). Analysis of resonance energy transfer in model membranes: Role of orientational effects. *Biophys. Chem.* **99**, 143–154.
14. M. L. Johnson (1983). Evaluation and propagation of confidence intervals in nonlinear, asymmetrical variance spaces. *Biophys. J.* **44**, 101–106.
15. M. L. Johnson (2000). Parameter correlations while curve fitting. *Meth. Enzymol.* **321**, 424–446.
16. J. R. Lakowicz (1999). *Principles of Fluorescence Spectroscopy*, 2nd ed., Kluwer Academic, New York.
17. J. M. Beechem and E. Haas (1989). Simultaneous determination of intramolecular distance distribution and conformational dynamics by global analysis of energy transfer measurements. *Biophys. J.* **55**, 1225–1236.
18. J. M. Beechem (1992). Global analysis of biochemical and biophysical data. *Meth. Enzymol.* **210**, 37–54.
19. Yu. V. Kholin, D. S. Konyaev, and S. A. Mernyi (1999). Construction of complexation models: From measurements to final verdict. *Kharkov Uni. Bull. No. 437, Chem. Ser.* **26**, 17–35.
20. L. Zekany and I. Nagypal (1985). *Computational Methods for the Determination of Formation Constants*, Plenum, New York.
21. J. G. Molotkovsky, P. I. Dmitriev, L. F. Nikulina, and L. D. Bergelson (1979). Synthesis of new fluorescently labeled phosphatidylcholines. *Bioorg. Khim.* **5**, 588–594.
22. Z. Gryczynsky, J. Lubkowski, and E. Bucci (1995). Heme-protein interactions in horse heart myoglobin at neutral pH and exposed to acid investigated by time-resolved fluorescence in the pico- to nanosecond time range. *J. Biol. Chem.* **270**, 19232–19237.
23. L. M. S. Loura, A. Fedorov, and M. Prieto (1996). Resonance energy transfer in a model system of membranes: Application to gel and liquid crystalline phases. *Biophys. J.* **71**, 1823–1836.
24. Q. Chen and B. R. Lentz (1997). Fluorescence resonance energy transfer study of shape changes in membrane-bound bovine prothrombin and meizothrombin. *Biochemistry* **36**, 4701–4711.